"*Release of aged contaminants from weathered sediments: Effects of sorbate speciation on scaling of reactive transport*"

Grant no. DE-FG02-08ER64615

(Joint Final Report with Grant no. DE-FG02-08ER64616)

8/15/2008-8/14/2012

Project Investigators: Jon Chorover and Nico Perdrial (University of Arizona); Karl Mueller and Caleb Strepka (Penn State University); Peggy O'Day and Nelson Rivera (University of California, Merced); Wooyong Um and Hyun-Shik Chang (Pacific Northwest National Laboratory); Carl Steefel (Lawrence Berkeley National Laboratory); Aaron Thompson (University of Georgia).

Hanford sediments impacted by hyperalkaline high level radioactive waste have undergone incongruent silicate mineral weathering concurrent with contaminant uptake (Chorover et al., 2008). In this project, we studied the impact of background pore water (BPW) on strontium, cesium and iodine desorption and transport in Hanford sediments that were experimentally weathered by contact with simulated hyperalkaline tank waste leachate (STWL) solutions. Using those lab-weathered Hanford sediments (HS) and model precipitates formed during nucleation from homogeneous STWL solutions (HN), we (i) provided thorough characterization of reaction products over a matrix of field-relevant gradients in contaminant concentration, P_{CO2}, and reaction time; (ii) improved molecular-scale understanding of how sorbate speciation controls contaminant desorption from weathered sediments upon removal of caustic sources; and (iii) developed a mechanistic, predictive model of meso- to field-scale contaminant reactive transport under these conditions. Below, we provide some detailed descriptions of our results from this three year study, recently completed following a one-year no cost extension.

1. Characterization of Contaminant Uptake

Characterization of STWL-sediment reaction products using EXAFS, NMR, EM and quantitative-XRD indicated the importance of waste chemistry on the kinetics and trajectory of mineral transformation during sediment contact (i.e., native silicates → zeolites → sodalite → cancrinite). The presence or absence of CO_2 during HN affected solid phase templating and growth of either zeolite X (no CO_2) or sodalite/cancrinite (with CO_2), both of which sequester nitrate, Sr and Cs into distinct sites (Rivera et al., 2011; Perdrial et al., 2011). After 1 month of aging, zeolite X (with a 1:1 ratio of Al to Si) was precipitated from low CO_2 solutions while high CO_2 solutions contained mixtures of zeolite X, sodalite, and cancrinite, with the latter being the dominant phase. Quantitative fits to high-resolution solid-state aluminum-27 MAS NMR spectra show that after 548 days of aging, the cancrinite fraction increases relative to zeolite X and sodalite (Table 1). Strontium EXAFS analysis (Figure 1) shows that in zeolite X, Sr predominantly occupies regular 6-coordinated sites between beta cages (30-day, low CO_2 samples for both Sr+Cs and Sr-only precipitates). In 548 day, high CO_2 samples, interatomic distances from EXAFS are consistent with Sr located in 12-membered rings of cancrinite. Results indicate that Sr and Cs occupy different sites within zeolite or feldspathoid cage structures, and that the presence of both contaminants changes the distribution of occupancy in cation sites.

Table 1. *Results of NMR peak deconvolution for 548 days aged solids at 11.7 T magnetic field.C: cancrinite, S:sodalite, Z: Zeolite (Rivera et al., 2011)*

Sample	ppm shift	Area (%)	ppm shift	Area (%)	ppm shift	Area (%)	ppm shift	Area (%)	Mineral phases*
548 d Sr+Cs +CO_2	58	10	60	50	62	30	66	10	C/S/Z
548 d Sr +CO_2	58	15	60	43	62	33	66	9	C/S/Z
548 d Cs +CO_2	58	9	60	47	62	32	66	13	C/S
548 d Na +CO_2	58	11	60	42	62	31	66	16	C/S

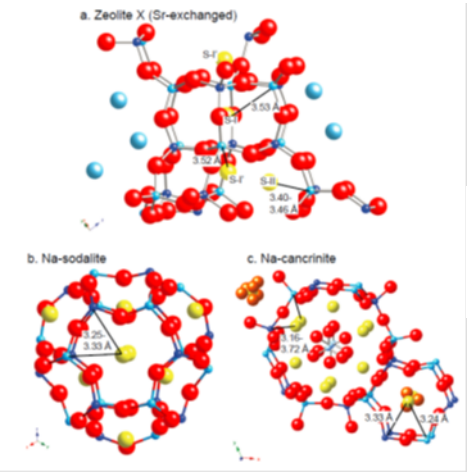

Figure 1. *Example cation sites (yellow atoms) and typical distances betwwen cations and framework Al (light blue) or Si (dark blue)atoms for a) Sr-exchanged zeolite-X; b) Na-sodalite; c) Na-cancrinite. (Rivera et al., 2011)*

In whole Hanford Sediments (HS) reacted with STWL, mineral transformations follow a similar path. Rietveld quantitative XRD analysis performed on sediments reacted at low and high contaminant concentrations, with and without atmospheric CO_2 shows that these STWL chemical parameters affect differences in silicate mineral transformations (Figure 2 – Table 2). In particular, low contaminant concentrations (LOW) favor the formation of sodalite and cancrinite at 185 days, whereas at high contaminant concentrations (HIGH) zeolite (chabazite) persists as the dominant neo-precipitate. Hence, despite being present at trace level relative to the principal mineral forming solutes (i.e., Si, Al, Na, Ca, CO_3, and NO_3) *contaminant concentration controls contaminant siting in secondary reaction products*. For example, EXAFS shows that Sr local coordination trends with variation in quantitative XRD of secondary reaction products (Table 3). In addition to LOW vs. HIGH effects, presence ($+CO_2$) or absence ($-CO_2$) of atmospheric P_{CO2} also affects incongruent silicate weathering in STWL-HS systems, primarily through its negative effect on calcite dissolution. This is significant because calcite Ca^{2+} release promotes strätlingite ($Ca_2Al_2SiO_2(OH)_{10}{\cdot}3H_2O$) formation under $-CO_2$ but not $+CO_2$ conditions. The associated depletion of aqueous Si and Al inhibits feldspathoid formation, thereby impacting Sr and Cs uptake and local coordination in product solids. These molecular-scale effects reverberate at the meso-scale to influence contaminant release kinetics in sediment columns (see next section).

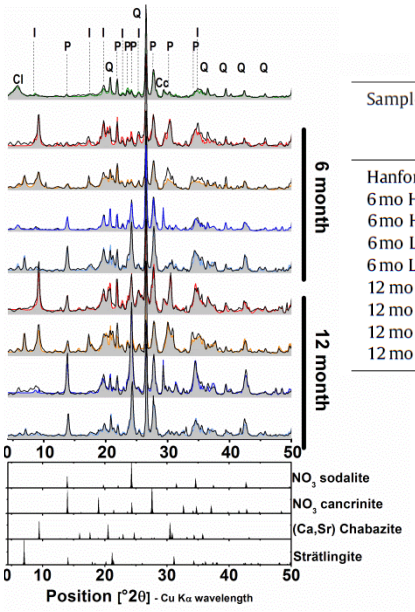

Sample name	Calcite $CaCO_3$	Sr,Ca chabazite $Ca_{1.4}Sr_{0.3}Al_{3.8}Si_{8.3}O_{24}{\cdot}13H_2O$	NO_3-sodalite $Na_8(AlSiO_4)_6(NO_3)_2$	NO_3-cancrinite $Na_{7.6}(AlSiO_4)_6(NO_3)_{1.6}(H_2O)_2$	Strätlingite $Ca_2Al_2SiO_7{\cdot}8(H_2O)$
Hanford	3.1	0.0	0.0	0.0	0.0
6 mo High $+CO_2$	1.4	14.2	0.0	0.0	0.0
6 mo High $-CO_2$	0.0	20.0	0.0	0.0	15.5
6 mo Low $+CO_2$	7.3	0.2	10.6	4.0	0.0
6 mo Low $-CO_2$	0.0	4.0	11.1	11.2	8.3
12 mo High $+CO_2$	2.2	13.9	8.8	3.7	0.00
12 mo High $-CO_2$	0.0	27.9	0.2	0.4	14.4
12 mo Low $+CO_2$	6.4	0.1	23.6	9.3	0.0
12 mo Low $-CO_2$	0.0	1.3	29.0	16.1	2.8

Table 3. *Linear combination fits in percent of components of Sr K-edge EXAFS spectra for fine fraction isolates (Perdrial et al., 2011).*

Sample	Unreacted Sediment [a]	Strontianite ($SrCO_3$) [a]	Sodalite/ cancrinite [a]	Chabazite [a]	Total
6 mo High [+CO_2]	0	29 ± 2	32 ± 4	42 ± 4	103 ± 6
6 mo High [-CO_2]	0	0	0	114 ± 4	114 ± 4
6 mo Low [+CO_2]	94 ± 5	0	13 ± 4	0	107 ± 7
6 mo Low [-CO_2]	67 ± 4	0	31 ± 3	0	98 ± 4
12 mo High [+CO_2]	0	49 ± 1	49 ± 2	0	98 ± 3
12 mo High [-CO_2]	0	0	0	112 ± 3	112 ± 3
12 mo Low [+CO_2]	85 ± 6	0	20 ± 4	0	105 ± 7
12 mo Low [-CO_2]	50 ± 6	0	48 ± 5	0	98 ± 8

Using a suite of methods (silver thiourea with Cs and Rb competition and flow-through technique with Rb), we measured the density of high affinity sites (HAS) in pristine and hyperalkaline-weathered Hanford sediments exposed to high or low concentrations of Cs, Sr and I for 6 months or 12 months under either CO_2-free or atmospheric CO_2 conditions. New mineral formation affected HAS density, with hyperalkaline-weathering of these sediments increasing the density of high affinity Cs and Rb adsorption sites relative to pristine Hanford sediments. More specifically, the formation of illite, feldspathoid, and zeolite in the reacted sediments altered Cs and Rb sorption. HAS density was greatest for the sediments weathered at HIGH contaminant concentration suggesting that zeolite products - formed preferentially in the HIGH treatments - produced more Cs and Rb HAS than did the formation of NO_3-feldspthoids, which formed preferentially the LOW treatments. Also, lower partial pressure of CO_2 ([-CO_2] treatments) during weathering increased the development of HAS. This could be due to the increase in "strätlingite [$Ca_2Al_2SiO_7 \cdot 8(H_2O)$]" formation that occurred preferentially in the [-CO_2] treatments.

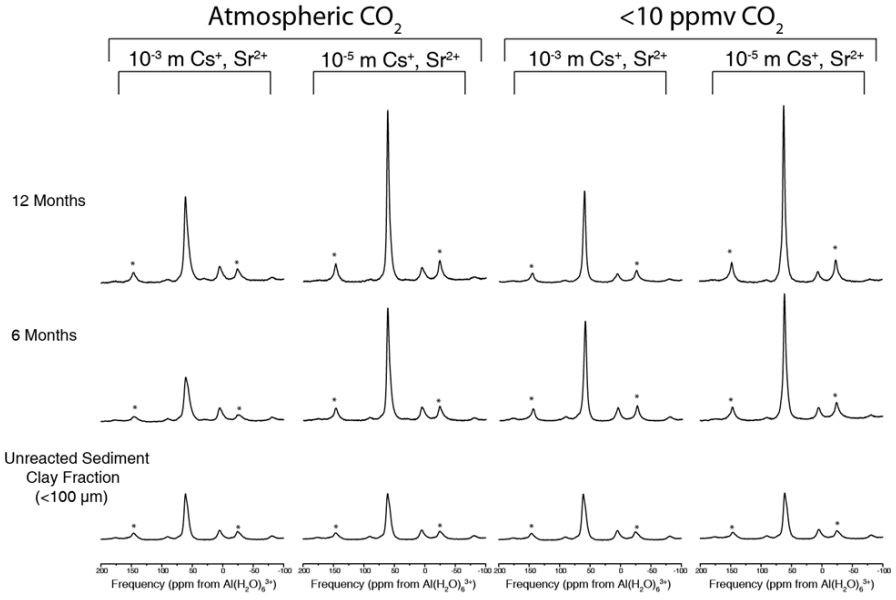

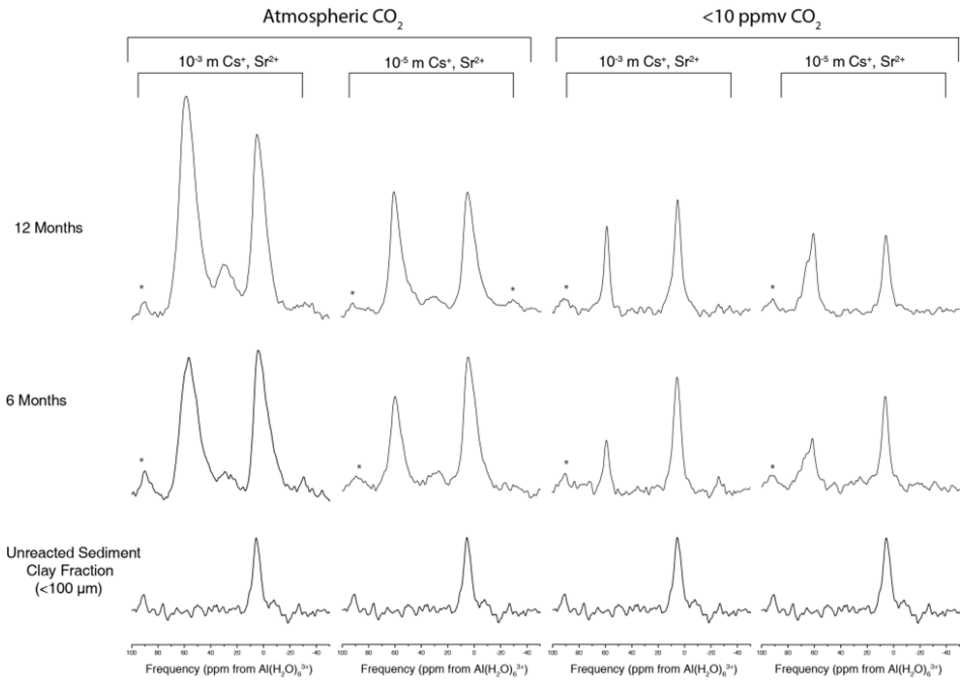

Figure 4. *Overview of $^{1}H/^{27}Al$ CPMAS NMR spectra for STWL weathered Hanford sediment.*

^{27}Al MAS data have been used to quantify the time-dependent formation of secondary phases (Figure 3). An increase in tetrahedrally coordinated species (-60 ppm) relative to octahedrally coordinated species (0 ppm) is observed with increasing weathering time. These results are supported by our ^{27}Al cross-polarization MAS (CPMAS) work (Figure 4), which has furthered our understanding of the conditions under which certain neophases form. Tetrahedral species present in the MAS spectrum of the unreacted sediment are not observed in the CPMAS spectrum, indicating that only octahedral species are initially collocated with protons. Neoformed tetrahedral species, collocated with hydrogen atoms, are observed with subsequent weathering. Some variation is observed in the formation of these species, with sediments weathered in the presence of CO_2 exhibiting a greater degree of proton-bearing aluminum neophase formation. No differentiation between tetrahedral species is seen, with the possible exception of sediment weathered in 10^{-5} m Cs and Sr in the absence of CO_2. Interestingly, samples weathered in the presence of CO_2 are observed to contain pentacoordinated aluminum in addition to the tetrahedrally coordinated and octahedrally coordinated species observed in direct polarization experiments.

Our NMR experiments have also focused on characterization of specimen minerals (including clays) and Hanford sediments reacted with synthetic tank waste leachate containing contaminant Cs and Sr (in non-radioactive forms) in batch weathering experiments.

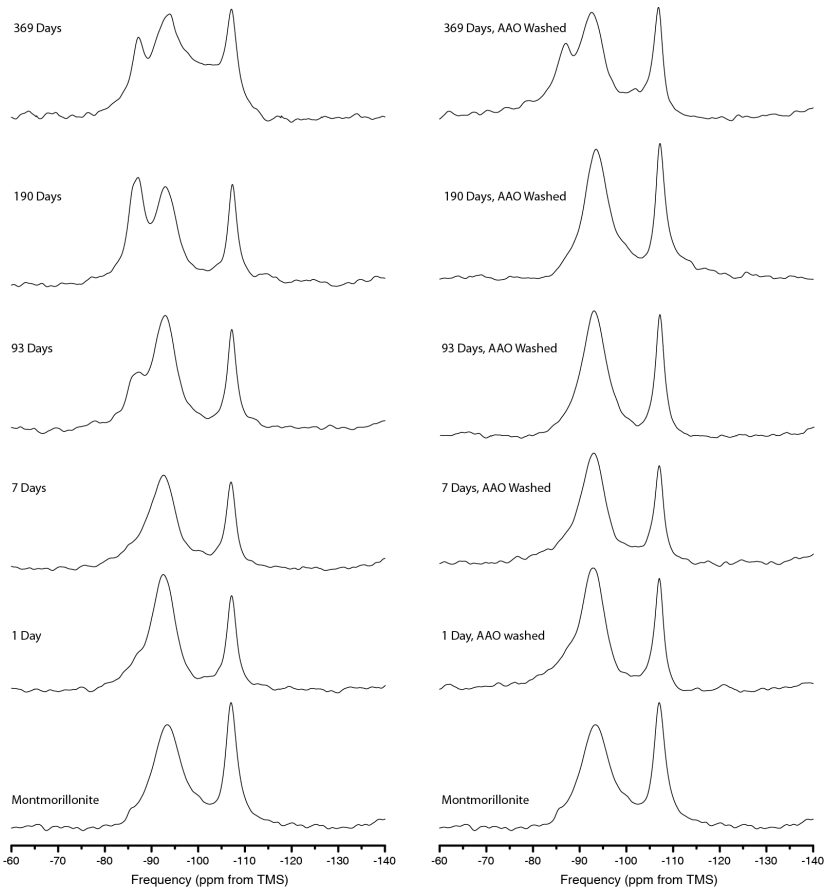

Figure 5. *^{29}Si MAS NMR spectra of montmorillonite (SWy-2), from the Source Clays Repository of the Clay Minerals Society, after reaction with a caustic STWL solution as well as subsequent AAO washes.*

A combination of ^{29}Si magic-angle spinning (MAS) and ^{1}H/^{29}Si double-resonance methods have extended our understanding of the effects of STWL-mediated weathering on montmorillonite clay. ^{29}Si MAS experiments provide a useful tool for quantitatively analyzing the formation of secondary phases (Figure 5). In these studies, resonances corresponding to montmorillonite (-93 ppm) and quartz (-108 ppm) are observed in the spectrum of the unreacted source clay. A neoformed silicate phase (-86 ppm) is observed after 93 days of reaction in STWL containing 10^{-3} m Cs and Sr contaminants, but this phase is not present after an acidic ammonium oxalate (AAO) wash to remove poorly crystalline phases. The intensity of this neophase resonance has increased after 190 days of weathering, but it is still not observed after an AAO wash. Of particular interest, a broad series of resonances (ranging from -96 to -105 ppm) is observed after 369 days of weathering. These phases are reduced, but not eliminated, after an AAO wash.

^{1}H/^{29}Si cross-polarization Carr-Purcell-Meiboom-Gill (CP-CPMG) MAS studies (Figure 6) have recently been introduced into our experimental protocol and provide valuable insight into the nature of the neophases in the montmorillonite studies. These experiments indicate which resonances are from species that are in a heavily protonated environment and allow observation in the absence of signal from phases present in the source clay. The only species observed in the unreacted source clay are a hydrated quartz-like phase (-107 ppm) and an unidentified minor phase (-100 ppm). Neophase formation (-86 ppm) is first seen after 93 days of reaction in STWL, and continues to increase after 190 days of weathering, indicating that these neoformed silicates either contain or are close to species containing protons. Removal of these phases with an AAO wash indicates that after 190 days silicate neophases are still poorly crystalline. A broad series of neophases (-90 to -110 ppm) is observed after 369 days of weathering. The spectrum of the AAO washed 369 day sample indicates that both neoformed species are recalcitrant.

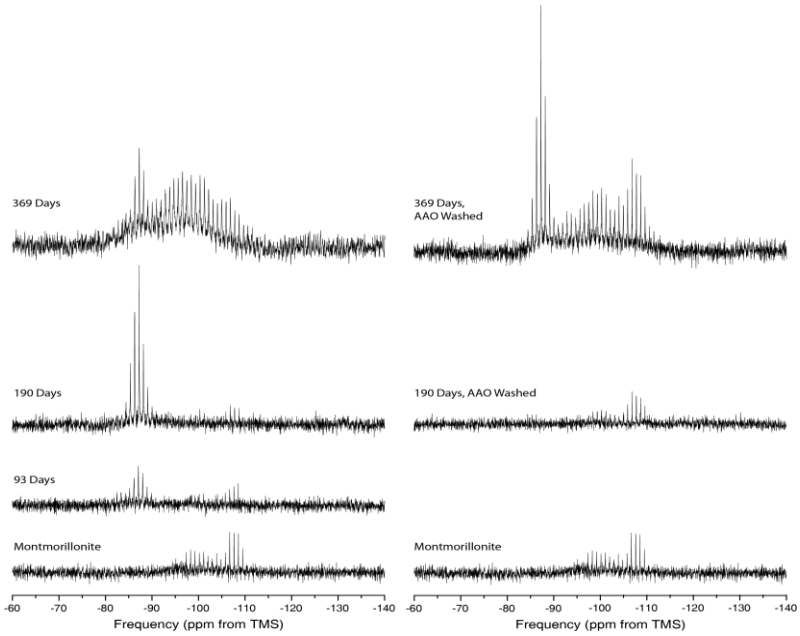

Figure 6. *$^{1}H^{29}Si$ CPCPMG-MAS NMR spectra of montmorillonite reacted with STWL provide information about silicon species in close spatial proximity to protons.*

2. Contaminant Desorption upon BPW Leaching

Saturated and unsaturated column experiments were conducted to assess the kinetics of contaminant desorption from HS and HN solid-phase reaction products upon leaching with Background Pore Water (BPW).

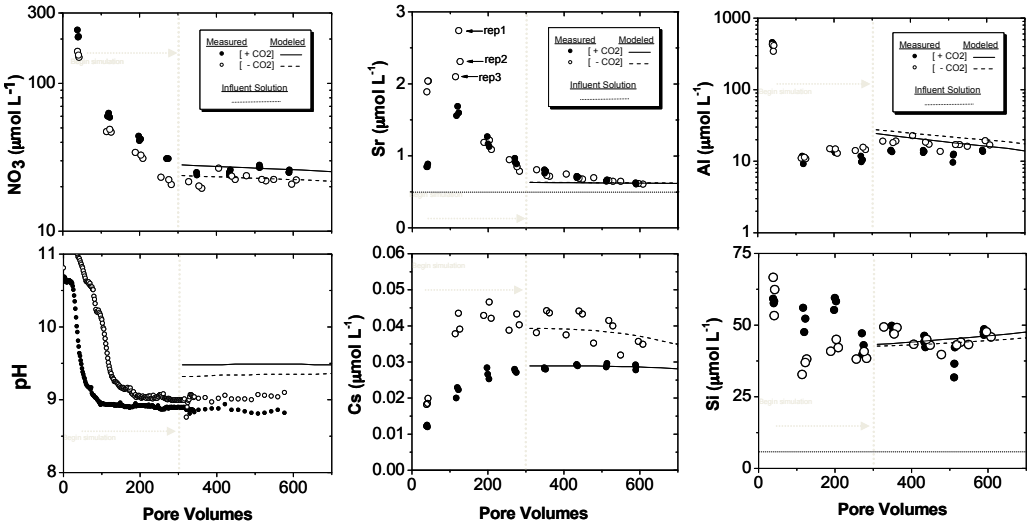

2.2.1 Hanford Sediments: For sediments weathered at low contaminant concentrations (LOW), reactive transport (CrunchFlow) modeling of HS column BPW effluents is consistent with rapid I desorption from a paucity of anion exchange sites, and slower Cs desorption from frayed edge sites on native illitic sediments, whereas Sr desorption was fit by neophase aluminosilicate dissolution assuming no ion exchange in feldspathoids (Figure 7, and Thompson et al., 2010). However, the model simulation in sediments weathered at high contaminant concentrations (HIGH) suggests that initial Sr release derives

from "planar" ion exchange sites. An abrupt release of Sr later in the leaching experiment (observed only in HIGH) might signal dissolution of a more crystalline mineral (e.g., cancrinite). Unstable amorphous mineral(s) dissolution in the early stage of BPW leaching is apparent and affects early contaminant release.

Long-term flow-through column experiments, where 365 d reacted sediments were leached by 800PV of BPW, showed that in comparison to the sediments reacted for 185 d, Cs release was diminished for the HIGH (9% vs. 12% [+CO_2] and 8.6% vs. 14.1% [-CO_2] as fraction of Cs uptake) and increased slightly for the LOW (8.8% vs. 8.0% [+CO_2] and 11.5% vs. 12.3% [-CO_2]). Conversely, in all cases, the mass of Sr released was diminished with increasing STWL reaction time. In LOW systems, NO_3 dissolution in BPW also decreased with increasing STWL reaction time. These results are consistent with our EXAFS results (Table 3) that show Sr being primarily sequestered into increasingly recalcitrant feldspathoids, whereas Cs is dominantly loaded on exchange sites and only slightly incorporated in the feldspathoids (in the LOW). The molar Si/Al ratio in BPW effluents ranges from 2 to 4. However, the Si/Sr ratio is more variable over the leaching period, suggesting heterogeneity in the dissolving neoprecipitate composition. Similarly the release of NO_3 in the LOW is not stoichiometric with Si suggesting that part of the NO_3 release is from anion exchange.

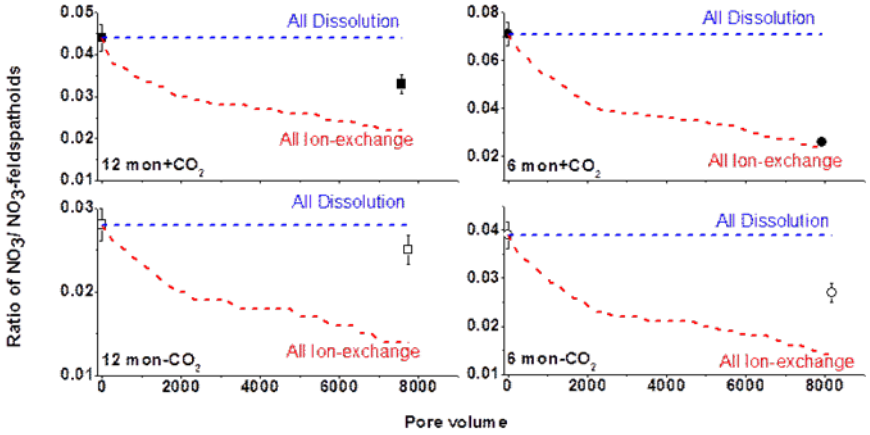

Figure 8. *Ratio of NO_3 release relative to the concentration of NO_3-feldspathoids in the sediments. (Deng et al. In Prep)*

Exhaustive leaching (for ~8000 PV) of all reacted sediments allowed us to discern the relative contributions of feldspathoid dissolution and anion exchange to total NO_3 desorption. Based on the assumption that Cs and Sr exist only as ion pairs with NO_3 in the NO_3-feldspathoids, the evolution of the ratio of NO_3 to NO_3-felspathoids abundance should be an indicator of the relative contributions of feldspathoid dissolution and anion exchange to total NO_3 desorption. The final ratio of the remaining NO_3 to the remaining NO_3-felspathoids of the treatments suggested the release of $CsNO_{3(aq)}$ or $Sr(NO_3)_{2(aq)}$ from the [12 mon-CO_2] treatment is mainly via NO_3-feldspathoid dissolution, while the release of $CsNO_{3(aq)}$ or $Sr(NO_3)_{2(aq)}$ from the [6 mon+CO_2] treatment is mainly via ion-exchange (Figure 8). The release of $CsNO_{3(aq)}$ or $Sr(NO_3)_{2(aq)}$ from [12 mon+CO_2] and [6 mon-CO_2] treatments is via both ion exchange and NO_3-feldspathoid dissolution. Results from this experiment suggest shorter weathering times and the presence of CO_2 [+CO_2] generate more exchangeable NO_3. Evidently, excess NO_3 accumulation above the final stable ratio (~0.025) is lost via ion exchange (up to 2000 PV); after reaching the stable final ratio 0.025, we predict NO_3 is released only via dissolution of the feldspathoid mineral phase.

Hanford sediments reacted for 12 months were also subjected to four 24 h dry/wet leaching cycles with BPW. After each drying event, large NO_3 pulses were observed in effluents, but these were not accompanied by corresponding Si pulses that would signal feldspathoid dissolution. Wetting-drying increased NO_3 desorption 4-5 fold over continuous flow experiments. Sr and Cs desorption is hampered in the dry/wet cycle experiments relative to continuous saturated or unsaturated flow, with more intense retardation when CO_2 was absent (Figure 9). In every case, pulsed release after drying events accelerated the desorption of iodine from the sediments. XRD characterization of the desorbed sediments after each

drying did not reveal any dissolution of either feldspathoids (LOW) or zeolites (HIGH), consistent with contaminant release being principally controlled by ion exchange.

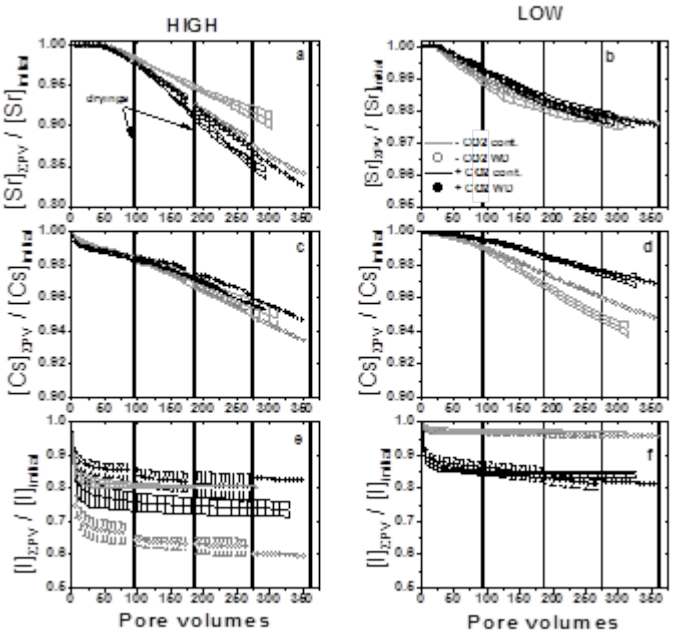

***Figure 9**. Evolution of Sr (top row), Cs (middle row) and I (bottom row) solid phase concentrations in the sediments during leaching, calculated from elemental release data. (Perdrial et al. In Prep a)*

In order to elucidate the processes responsible for the limited contaminant release, microscopic (TEM - XRD) and molecular scale (Sr-EXAFS) investigations of sediments subjected to moisture cycling flow-through desorption/dissolution experiments were performed. Important differences between the various treatments were observed. Under LOW conditions, only minor solid phase transformations were observed with extensive BPW leaching. Structural data extracted from quantitative synchrotron XRD of the sediments for HIGH conditions revealed mineral transformation and evolution of the local structure surrounding Sr and potentially Cs (distorsion of the zeolite cages and isomorphic transformation of chabazite to willhendersonite). Linear combination fits and shell-by-shell analyses performed on Sr K-edge EXAFS data (Table 4) are in good agreement with XRD quantification and structural observation indicating concentration dependent solid-state changes in Sr speciation. The increase in Sr-Si/Al distance within the zeolite cage provides a molecular-level explanation of the observed macroscale behavior.

Sample	Native sediment	Strontianite	Sodalite/ Cancrinite	Chabazite	Willhendersonite	Sum of components	Red. χ^2
$HIGH_{[+CO2]}$[a]	-	49 (1)	49 (2)	-	-	98 (3)	-
$HIGH_{[+CO2]}$ CF.[b]	8 (5)	-	28 (5)	36 (0.03)	38 (0.04)	110 (17)	0.13
$HIGH_{[+CO2]}$ 4WD[c]	19 (5)	-	22 (6)	42 (0.03)	37 (0.04)	120 (18)	0.15
$HIGH_{[-CO2]}$[a]	-	-	-	112 (0.03)	-	112 (3)	-
$HIGH_{[-CO2]}$ CF.	23 (4)	-	32 (5)	31 (0.02)	29 (0.03)	115 (14)	0.09
$HIGH_{[-CO2]}$ 4WD	33 (5)	-	27 (5)	33 (0.03)	22 (0.04)	115 (17)	0.13
$LOW_{[+CO2]}$[a]	85 (6)	-	20 (4)	-	-	105 (10)	-
$LOW_{[+CO2]}$ CF.	53 (7)	32 (7)	32 (6)	-	-	117 (20)	0.43
$LOW_{[+CO2]}$ 4WD	47 (3)	18 (3)	41 (3)	-	-	106 (90)	0.10
$LOW_{[-CO2]}$[a]	50 (6)	-	48 (5)	-	-	98 (8)	-
$LOW_{[-CO2]}$ CF.	79 (5)	-	21 (5)	-	-	100 (10)	0.48
$LOW_{[-CO2]}$ 4WD	67 (5)	-	36 (3)	-	-	103 (8)	0.18

(a) Data from Perdrial et al. (2011).; (b) CF. stands for continuous flow-through leached sample. ; (c) 4WD stands for leached samples after four wet-dry cycles.

According to the cleanup plans for the Hanford site, waste tanks are scheduled to be removed and the subsurface matrix will be returned to physical and chemical environments characteristic of natural recharge of dilute pore water at circumneutral pH. In the subsurface environment, the transport of colloids in aqueous suspension is generally believed to be mainly influenced by media water content, fluid flow rate and flow pattern, ionic strength, and pH of the pore water (Kaplan et al., 1993; Roy and Dzombak, 1997; Gamerdinger and Kaplan, 2001; Um and PaPelis, 2002; Ryan and Gschwend, 1994; Zhuang et al., 2007). Therefore, information regarding the stability or remobilization of radionuclide-containing secondary precipitates under changed physicochemical conditions of the background solutions in the future subsurface environment is needed in order to forecast transport and to conduct a long-term safety performance assessment in Hanford site after tank closure. In order to quantify the amount of contaminant release that may be associated with colloidal and particulate transfer from saturated analog sediments we monitored the concentrations of major and trace (including Sr, Cs and I) elements effluent from analog sediment columns leached with BPW containing different filter sizes. The nature and crystalline composition of the particles leached out was monitored by electron microscopy and x-ray diffraction. The objectives of that work was to i) quantify the contribution of particle and colloid facilitated transport of contaminant on the total release of contaminant and ii) verify the validity of aqueous transport models based on effluent concentrations from solutions filtered at 0.45 μm.

Table 5: *Contribution of the different fractions to contaminant release ($\mu mol\ L^{-1}$). Standard deviation in brackets*

	Truly dissolved (<0.025 μm)			Colloidal (0.025 to 0.450 μm)			Particulate (0.45 to 20.00 μm)		
	Sr	Cs	I	Sr	Cs	I	Sr	Cs	I
LOW	15.1 *(0.6)*	0.13 *(0.01)*	1.98 *(0.53)*	0.41 *(0.61)*	0.03 *(0.01)*	0.004 *(0.53)*	0.80 *(1.02)*	-0.001 *(0.01)*	0.19 *(0.09)*
HIGH	250.7 *(7.8)*	15.9 *(0.96)*	3.00 *(0.22)*	23.3 *(7.8)*	0.63 *(0.96)*	-1.21 *(0.22)*	46.1 *(18.9)*	0.54 *(0.39)*	0.85 *(0.31)*

The contributions of three fractions to contaminant transfer at the end of the experiment are displayed in **Table 5**. Contaminants were mostly released in TD form. In the LOW neither the colloidal or particulate fractions significantly contributed to contaminant release. Conversely, in the HIGH, colloidal Sr, and particulate releases of all contaminants were significant. Release curves revealed that each contribution varied during leaching. A correlation between particulate Ca and Sr was observed. The amount of materials deposited on the 0.45 um filter was higher for the HIGH (1.0 $g.kg^{-1}$ soil) than for the LOW (0.2 $g.kg^{-1}$ soil). SEM/EDS observation showed that most of the particles released from HIGH were Sr/Cs-containing zeolites, with smaller amounts of feldspathoids of similar composition but smaller counts for Sr and no Cs detected. In the LOW, particles were mostly feldspathoids with a composition similar to that of the HIGH but no detectable Sr. XRD quantification of the filter retentate revealed that 50% of the particulate matter was zeolitic and 25% was feldspathoidic in the HIGH, and 50% was feldspathoidic and 25% micaceous in the LOW.

Colloids deposited on the TEM grids consisted of aggregates of ball-shaped veils in the HIGH and the LOW. EDS/SAED analysis revealed that they were amorphous zeolitic precursors with no detectable Sr, Cs or I (**Figure 10**). The Si/Al ratio was generally >1 in the HIGH and <1 in the LOW. Results showed that particulate transport of contaminants is potentially significant from sediments reacted with millimolar levels of contaminants, zeolites being their primary carrier, whereas colloidal transport did not appear to be significant.

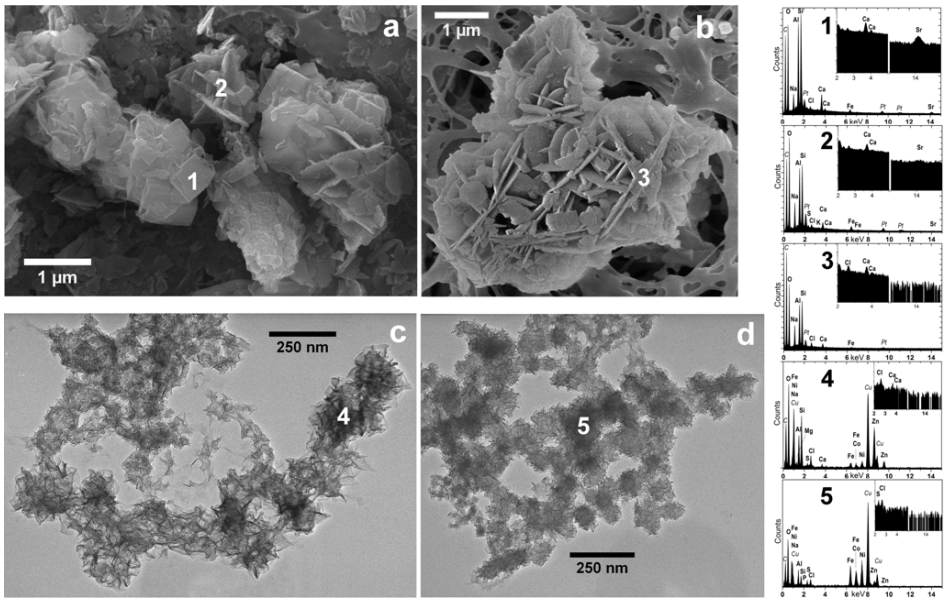

Figure 10. *Selected EM images of the particles released during BPW leaching of the a) HIGH filtered at 20 µm, b) LOW filtered at 20 µm, c) HIGH filtered at 0.45 µm, d) LOW filtered at 0.45 µm. a) and b) are SEM images and c) and d) are TEM images. Numbers on the images correspond to the EDS analyses displayed on the right of the images. Labels in italics on the spectra denote artifacts due to the support of the samples. (Perdrial et al. In Prep c)*

In addition to these transient-flow colloidal and particulate release experiments from complex sediments, columns were packed with two different colloid-sized precipitates-containing sand materials, generated using either batch (named "BR material") or column (named "CR material") experiments by reacting quartz sand with a simulated tank waste leachate (STWL, Sr was added as the target radionuclide) at 89°C. The neo-formed secondary precipitates in both BR and CR materials were identified by XRD, SEM, and EDS to be nitrate-cancrinite. During the column leaching, flow rates, solution ionic strength or pH was stepwise changed to evaluate the remobilization of the Sr-containing neo-formed precipitates under potentially changed background conditions in the subsurface. In addition, batch cation exchange experiments were also conducted to determine the Sr mass distribution between the surface-adsorbed and co-precipitated in the neo-formed nitrate-cancrinite mineral.

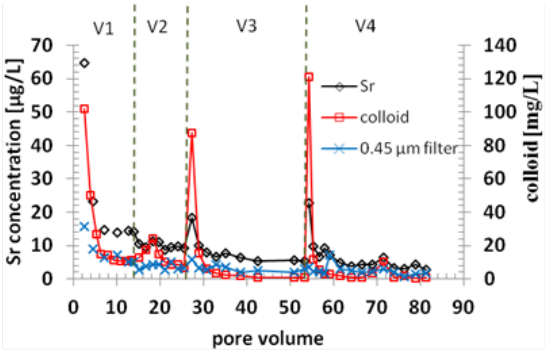

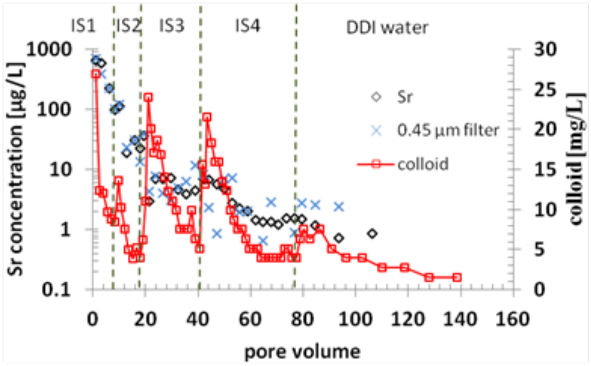

Results of these column experiments suggest that the neo-formed secondary precipitates (sodalite and cancrinite) at the Hanford site could behave like normal native colloids which can facilitate

radionuclide transport. Initially immobilized radionuclide-containing precipitates could be remobilized given a change of background geochemical conditions. Figures 11 & 12 show examples of enhanced colloid and Sr transport under changed flow rate, solution ionic strength, and pH. In this study, the remobilization of neo-formed nitrate-cancrinite precipitates was strongly dependent on geochemical conditions, primarily ionic strength and pH of the background solution, as well as the flow rate. The re-mobilization of neo-formed precipitates increased with increase of the leaching solution flow rate due to the increased hydrodynamic shear applied to colloids. The re-mobilization of the neo-formed precipitates also increased with decreasing solution ionic strength and increasing pH, because of the increase in repulsive electrostatic force between colloid-sediment interfaces, consistent with DLVO theory. Our independent ion exchange experiment indicated that substantial Sr mass was co-precipitated inside the nitrate-cancrinite structures, which enhanced the impact of colloid remobilization on Sr transport. However, at higher ionic strength, despite decreased colloid concentration and transport, the adsorbed Sr can be released into solution through ion exchange processes. Therefore, both mobilization neo-formed precipitates and ion exchange processes could contribute to Sr transport, and the impact of both processes depend on geochemical conditions.

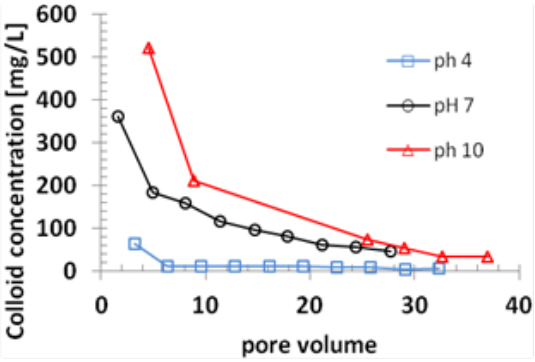

Figure 12*. pH effect on colloid breakthrough curves from 3 identical BR material-packed columns using 0.005M $NaNO_3$ solutions with different pH (=4, 7, and 10) at a constant flow rate of 0.03 mL/min. (Wang & Um. In Prep)*

2.2.2 Homogeneous Nucleation (HN) Products: Quartz columns were amended with HN precipitates that had been aged for 30 d in degassed solutions (low-CO_2) in which the solid phase was predominately zeolite X. These columns were then leached with BPW in model system studies designed to help constrain whole sediments studies. Cesium was quite readily desorbed (up to 40% of total Cs in solids), while only 6% of the Sr was released to solution. A reactive transport model (Crunchflow) was developed to describe Sr and Cs release from the previously characterized solid phases (Rivera et al., 2011). Parameter estimation was performed (using the program PEST) to derive a set of selectivity coefficients describing exchange sites on both zeolite and feldspathoid phases, in addition to dissolution of solid HN phases. Ion exchange site identities and concentrations were constrained by mineral structure and site occupancies determined in our prior characterization. The reactive transport model was calibrated on experiments with Sr and Cs as individual contaminants to generate a set of ion exchange constants describing competition among all monovalent and divalent cations. The transferability of the model was then tested on desorption experiments with HN solids containing both Sr and Cs as co-contaminants.

Modeling of the experimental effluent concentrations indicated that the dominant mechanism of release of Sr and Cs is ion exchange, rather than dissolution of aluminosilicate neophases, appears to be the dominant driving force for release of Sr and Cs based on the total amount of Si and Al released (~ 1% of total in solids). For precipitates aged for 548 days with CO_2 present (predominately cancrinite/sodalite), 6% and 14% of total Sr and Cs, respectively, were desorbed in column experiments with Sr or Cs as a single contaminant. With Sr+Cs present as co-contaminants, up to 45% of total Sr was desorbed while only 8% of total Cs was removed. Differences in Sr and Cs release can be accounted for by the fraction of Sr strongly bound in inter-cage sites in zeolite X versus competition between Sr and Cs for exchangeable cage sites in cancrinite. Results from HN column experiments and quantitative XRD and NMR of BPW-leached HS samples suggest that contaminant desorption from the neoformed zeolites

and feldspathoids can also occur via ion exchange with minimal feldspathoid dissolution or phase interconversion. Hence, ion exchange reactions of contaminants within the neo-precipitates themselves need to be incorporated into future versions of the transport model.

3 Reactive-Transport Modeling of Contaminant Desorption

Our results indicate that STWL composition, P_{CO2}, and reaction time strongly influence contaminant sequestration mechanisms and, therefore, the rate and extent of subsequent re-mobilization and transport in Hanford vadose zone sediments. Our efforts to adapt Crunchflow to these column desorption studies focused initially on the steady-state desorption behavior that emerges at ca. 300 PVs. Here our current model invokes incongruent feldspathoid dissolution with the potential for aluminum hydroxide and aluminosilicate precipitation to match effluent NO_3 concentrations. In the LOW treatments, Sr substitution of less than 0.2% of the Na in the dissolving feldspathoid is necessary to reproduce the Sr effluent concentrations. The HIGH treatments—which had much lower feldspathoid neoformation and hence lower NO_3 desorption—require an additional Sr source. There is little thermodynamic driving force for zeolite dissolution (based on current published thermodynamic datasets) and our HN experiments suggest ion exchange rather than zeolite dissolution, so we are adapting our model for Sr and Cs ion exchange on the zeolites. In the early, transient desorption period (<200 PVs), these steady-state model formulations are supplemented with ion exchange on the bulk illitic materials and additional mineral dissolution reactions to accommodate a rapid efflux of ions in the earliest PVs. In addition, we are measuring the density of frayed-edge-sites (FES) on each of the reactive sediments to reduce the number of fitted parameters in the model. In the current transient period model Sr and Cs desorption can be accurately described by Ca^{2+} displacement of Sr^{2+} and K^+ displacement Cs^+ from ion exchange models with FES and generalized planar exchange sites. However, fitting these desorption curves requires accurate model representation of the evolving milieu of aqueous ions—including the contaminant I — resulting from the concurrent dissolution of labile minerals formed during the sediment weathering processes. In our unsaturated-column experiments, a two site ion-exchange model was sufficient to simulate Cs desorption in the LOW treatments, whereas a three-site model was required in the HIGH treatment.

4. Conclusions

Results from the homogeneous nucleation experiments corroborate prior work highlighting the different behavior of Sr and Cs in reaction of STWL with Hanford sediments. Uptake and incorporation of Sr into zeolite and feldspathoid neophases and aging in the presence of STWL increases Sr retention by sediments during flushout by neutral BPW. The presence of dissolved K in the STWL solution strongly competes with Cs for sorption sites on sediments, resulting in both less Cs uptake from solution during reaction and more Cs release during flushout for the same reaction time. These results are consistent with Cs sorption associated primarily with phyllosilicate edge sites (clay and mica phases), and no major differences in Cs retention with reaction times up to 4 months. Increasing Sr retention with longer STWL reaction times reflects the formation and aging of aluminosilicate neophases that incorporate Sr, progressing from zeolite-type to feldspathoid-type phases with time. Examination of Sr and Cs uptake and release under dynamic conditions in column experiments demonstrates how variability in the extent of initial reaction of sediments with caustic wastes and aging time, together with differences in waste composition, can influence subsequent contaminant desorption behavior in neutral groundwater.

Characterization and quantification of mineralogical transformations and associated contaminant sequestration in complex sediments provided insight needed for prediction of contaminant stability subsequent to the waste source removal. For example, at atmospheric P_{CO2}, the precipitation of stable Sr and Cs containing feldspathoids occured after 12 mo of reaction at high contaminant concentrations, whereas in the absence of CO_2, chabazite remained dominant, resulting in effective contaminant sequestration and slower subsequent desorption. In samples with low contaminant concentration,

formation of mixed sodalite and cancrinite leads to effective stabilization of contaminant (Sr). A key observation of this study was that variation in concentrations of trace contaminant cations directs the trajectory of neoprecipitate formation and contaminant fate in caustic systems.

In order to assess the long-term persistence of the neoprecipitates for conditions where sediment pore water is again fed by rainwater recharge after removal of the caustic source, we leached the weathered sediments with dilute, neutral pH solutions. An important result of our study is that whatever the condition of waste-sediment reaction employed, contaminant (Sr, Cs and I) release remains very limited upon removal of the contaminant source.

Long-term (600 PV) saturated leaching experiments and short term (200 PV) unsaturated leaching experiments of 6 month weathered sediments and associated CrunchFlow simulations illustrates the need to incorporate mineral dissolution into conceptual and numerical models of (at least) Sr desorption under future Hanford site closure scenarios. We observed that the dissolution of feldspathoids formed during the reaction of liquid waste with siliceous sediments can serve as a long-term source of Sr desorption. Because these dissolution processes are likely active during all stages of sediment leaching, we suggest that future modeling efforts should include a mineral dissolution component even when shorter-term ion exchange processes dominate. Our results also suggest that ion exchange remains a dominant process governing Cs dynamics even after considerable leaching.

Similar leaching experiments performed on 1 year reacted sediments (saturated and wet-dry cycling, 300 PV) did not reveal significant dissolution of the neoprecipitates. Results suggested that the main mechanisms for contaminant release were a combination of ion exchange and mineral transformation. At the molecular scale, chabazite transformation into the isomorphic willhendersonite led to a continuum in sequestration of Sr (and Cs). *Therefore, Ostwald ripening of the neophase precipitates formed during STWL-sediment interaction affects the mechanmisms of subsequent contaminant release during BPW infiltration into waste-weathered sediments*. Our assessment of particulate and colloidal contribution to contaminant release showed that upon removal of the contaminant source, modification of the geochemical conditions (i.e. pH, ionic strength) triggers significant release of particle-associated Sr, Cs and I, particularly from areas were the waste derived contaminant concentrations were highest.

Dissertation supported by this award.

Strepka, C. (2010) – Solid-State NMR Studies of the Impact of Tank Waste Leachates in the Environment. Ph.D. Dissertation, Chemistry, Pennsylvania State University.

Rivera, N.A. (2011) – Sequestration and Release Mechanisms of Strontium and Cesium in Zeolite/Feldspathoid Systems and Laboratory Reacted Hanford Sediments. Ph.D. Dissertation, Environmental Systems, University of California, Merced.

Deng, Yi-Ting. (2012) – Assessing the Role of High Affinity Sorption Sites in Cesium Desorption from Hyperalkaline-Weathered Hanford Sediments. M.S. Thesis. University of Georgia.

Publications resulting from this work.

Chang H.-S., Um W., Rod K., Serne R.J., Thompson A., Perdrial N., Steefel C.I. and Chorover J. (2011) – Strontium and cesium release mechanisms during unsaturated flow through waste-weathered Hanford sediments. *Environmental Science and Technology*, 45, 8313-8320.

Chorover, J., S. K. Choi, P. Rotenberg, R. J. Serne, N. Rivera, C. Strepka, A. Thompson, K. T. Mueller, and P. A. O'Day, (2008) – Silicon Control of Strontium and Cesium Partitioning in Hydroxide-Weathered Sediments. *Geochimica et Cosmochimica Acta* **72**, 2024-2047.

Deng, Y.-T., Perdrial N. and Thompson A. (In Prep a). – Contaminant and nitrate desorption during three-month leaching of hyperalkaline-weathered Hanford sediments. For submission to: *Environmental Science and Technology*.

Deng, Y.-T., Schroeder, P., Steefel, C., Thompson, A. (In Prep b) – Alteration of high-affinity cesium sorption sites following hyperalkaline weathering of Hanford sediments. For submission to *Environmental Science & Technology*.

Perdrial N., Rivera N., Thompson A., O'Day P.A. and Chorover J. (2011) – Trace contaminant concentration affects mineral transformation and pollutant fate in hydroxide-weathered Hanford sediments. *Journal of Hazardous Materials*, 197, 119-127.

Perdrial N., Thompson A., Deng Y.-T., O'Day P. and Chorover J. (In Prep a). Moisture cycling effects on contaminant release from lab-weathered Hanford sediments: I. Contaminant release dynamics. For submission to: *Chemical Geology*

Perdrial N., Thompson A., O'Day P. and Chorover J. (In Prep b). Moisture cycling effects on contaminant release from lab-weathered Hanford sediments: II. Coupling of mineralogical transformation to contaminant solid-phase speciation. For submission to: *Chemical Geology*

Perdrial N., Thompson A. and Chorover J. (In Prep c). Quantifying particulate and colloidal release of radionuclides from saturated analog Hanford sediments. For submission to: *Environmental Science and Technology*.

Rivera N., Choi S., Strepka C., Mueller K., Perdrial N., Chorover J. And O'Day P.A. (2011) – Cesium and strontium incorporation into zeolite-type phases during homogeneous nucleation from caustic solutions. *American Mineralogist*, 96, 1809-1820.

Rivera, N., Perdrial, N., Chorover, J. and O'Day, P. A. (in prep. a) Dynamics of Sr and Cs sequestration and release in Hanford sediments reacted with caustic waste in column simulations. For submission to: *Geochemical Transactions*.

Rivera, N.A., Kanematsu, M., Steefel, C.I., Chorover, J., and O'Day, P. A. (in prep. b) Reactive transport modeling of Sr and Cs release from aluminosilicate neophases formed from caustic waste.

Rod, K.A., Um, W. and Flury, M. (2010) – Transport of strontium and cesium in simulated Hanford tank waste leachate through quartz sand under saturated and unsaturated flow. *Environmental Science and Technology,* 44, 8089-8094.

Thompson A., Steefel C.I., Perdrial N. and Chorover J. (2010) – Contaminant desorption during long-term leaching of hydroxide-weathered sediments. *Environmental Science and Technology*, 44, 1992-1997.

Wang G. and Um W. (Accepted) – Mineral dissolution and secondary precipitation on quartz sand in simulated Hanford tank solutions affecting subsurface porosity. *J. Hydrology*.

Wang G. and Um W. (In Prep) – Facilitated Sr Transport by Remobilization of Sr-containing secondary precipitates in Hanford site subsurface. For submission to: *Environmental Science and Technology*.

Presentations resulting from this work.

Chorover, J., Perdrial, N., O'Day, P. A., Rivera, N., Mueller, K. T., Strepka, C., Um, W., Chang, H.S., Steefel, C., and Thompson, A. (2010) Release of aged contaminants from weathered sediments: Effects of sorbate speciation on scaling of reactive transport. Invited presentation, DoE/ERSP Annual PI meeting, March, 2010, Washington DC.

Chorover, J. (2011) Pore scale processes and their impacts on contaminant transport in weathering systems. Invited presentation, DoE Subsurface Biogeochemistry Research (SBR) Program, Annual PI meeting, April 2011.

Chorover, J. (2012) Linking carbon flow to weathering in subsurface biogeochemical research. Invited presentation, DoE SBR Program, Annual PI meeting, April 2012.

Deng, Y-T., Perdrial, N. and Thompson, A. (2011) – Assessing Frayed-Edge Site Density and Contaminant Desorption In Hyperalkaline-Weathered Hanford Sediment. *Annual Meeting of Soil Science Society of America*, San Antonio, TX. October 19, 2011.

Mueller K.T. (2008) – Surface-Mediated Processes in the Environment: Enhancing Surface-Sensitive Solid-State NMR Methods with Computational Studies and Cyberinfrastructure. Department of Chemistry, Louisiana State University, Baton Rouge, Louisiana.

Mueller K.T. (2008) – Surface-Mediated Chemistry in Environmental and Materials Research: Solid-State NMR Coupled with Computations and Cyberinfrastructure. National Science Foundation (Chemistry Division), Arlington. Virginia.

Mueller K.T. (2008) – Solid-State NMR of Complex Materials and Their Surfaces: Fifteen Years of Connecting the Dots. *236th ACS National Meeting*, Philadelphia, Pennsylvania.

Mueller K.T. (2008) – Surface-Mediated Processes in the Environment: Enhancing Surface-Sensitive Solid-State NMR Methods with Computational Studies and Cyberinfrastructure. Department of Chemistry, Howard University, Washington, DC.

Mueller K.T. (2008) – Surfaces in the Environment: New Views using NMR and Computational Chemistry. Department of Chemistry, Old Dominion University, Norfolk, Virginia.

Mueller K.T. (2009) – Release of Aged Contaminants from Weathered Sediments: Effects of Sorbate Speciation on Scaling of Reactive Transport. *ERSP 4th Annual PI Meeting*, Lansdowne, Virginia.

Mueller K.T. (2009) – Chemical Reactivity in the Environment: Studies Incorporating Solid-State NMR Solutions. Department of Chemistry, Stony Brook University, Stony Brook, New York.

Mueller K.T. (2009) – Solid-State NMR and Surface-Mediated Processes in the Environment. Environmental Molecular Sciences Laboratory, Pacific Northwest National Laboratory, Richland, Washington.

Mueller K.T. (2009) – Surfaces in the Environment: New Views using NMR and Computational Chemistry. Department of Chemistry, Old Dominion University, Norfolk, Virginia.

Mueller K.T. (2009) – Solid-State NMR of Complex Materials and Their Surfaces: Sixteen Years of Connecting the Dots. *Nuclear Magnetic Resonance Symposium on Applications of High-field NMR*, Department of Chemistry, Penn State University, University Park, Pennsylvania.

Mueller K.T. (2010) – Solid-State NMR and Surface-Mediated Processes in the Environment. Department of Chemistry, Washington State University, Pullman, Washington.

Mueller K.T. (2010) – How Exceptional is Solid-State NMR. *52nd Rocky Mountain Conference on Analytical* Chemistry, Snowmass, Colorado.

Mueller K.T. (2010) – Approaching Environmental Chemistry at Oxide Surfaces using Solid-State NMR. *2010 Meeting of the International Chemical Congress of Pacific Basin Societies*, Honolulu, Hawaii.

Mueller K.T. (2011) – Solid-State NMR Applications in Surface Chemistry: Advances in Environmental and Energy Science. *Department of Chemical Engineering Seminar*, University of California, Berkeley, California.

Mueller K.T. (2011) – Solid-State NMR Applications in Surface Chemistry: Advances in Environmental and Materials Science. *Department of Materials Science and Engineering*, Rutgers University, Piscataway, New Jersey.

Mueller K.T. (2011) – Capabilities and Directions for Discovery using Magnetic Resonance at EMSL. *Department of Energy, Office of Biological and Environmental Sciences*, Germantown, Maryland.

Mueller K.T. (2011) – Coupling Solid-State NMR and Computational Approaches for Discovery: A Chemical Physics View of Complex Materials and Their Surfaces. *Department of Physics, University of Warwick*, Coventry, United Kingdom.

Perdrial N., Thompson A. and Chorover J. (2009) – Effects of mineral transformation, contaminant concentration and CO_2 pressure on contaminant speciation and mobility in simulated Hanford sediments. *46th Annual Meeting of the CMS*, June 5-11, Billings, MT, USA.

Perdrial N., Thompson A. and Chorover J. (2010) – Mineral transformations and contaminant release dynamics under wetting-drying cycles in simulated Hanford sediments. *Goldschmidt Conference*, June 13-18, Knoxville, TN, USA.

Perdrial N., Thompson A., Rivera N., Deng Y.-T., O'Day P. and Chorover J. (2011) – Predicting the fate of radionuclides at the Hanford tank farm using analog sediments. *Goldschmidt Conference*, August 14-19, Prague, Czech Rep.

Perdrial N., Thompson A. and Chorover J. (2011) – Quantifying particulate and colloidal release of radionuclides from analog Hanford sediments. *Fall Meeting, AGU*, Dec 5-9, San Francisco, CA, USA.

Perdrial N., O'Day P. and Chorover J. (2012) – Strontium fate in Hanford sediments – A multi-scale synchrotron X-Ray investigation. *SSRL/LCLS Users' Conference*, Oct 3-6, Menlo Park, CA, USA.

Rivera, N., O'Day, P. A., Choi, S., Thompson, A., and Chorover, J. (2008) Strontium and cesium desorption from reacted Hanford sediments. *18th Annual V.M. Goldschmidt Conference*, Vancouver, BC.

Rivera, N., O'Day, P. A., Choi, S., and Chorover, J. (2009) Mechanisms for sequestration and release of strontium and cesium in caustic waste-reacted sediments and precipitated phases, and implications for long-term contaminant retention. *DOE-ERSP Annual Principal Investigator Meeting*, Lansdowne, VA, April 20-23.

Strepka C., Choi S., O'Day N., Perdrial N., Chorover J. and Mueller K. (2009) – ^{27}Al NMR studies of the impact of tank waste leachates on Hanford sediments samples. *Goldschmidt Conference*, June 21-26, Davos, Switzerland.

Thompson A., Steefel C., Perdrial N. and Chorover J. (2010) – Transient-stage (<200 PV) modelling of Sr, Cs and I desorption from hyper-alkaline weathered Hanford sediments. *ASA, CSSA & SSSA Int. annual meeting*, Oct 31 - Nov 4 2010, Long Beach, CA, USA.

Um, W., Rod, K., Flury, M., Choi, S. and Choi, J. (2011) – The effects of secondary precipitates on transport of strontium and cesium with varying water contents at the Hanford Site. *Migration*, September 20-25, Kennewick, WA.

Um, W. and Chang, H.-S. (2011) – Release mechanisms of Sr and Cs from the weathered Hanford sediments. *Goldschmidt Conference*, August 14-19, Prague, Czech Rep.

Wang, G, and Um. W. (2011) – Radionuclide immobilization and flow path modifications by dissolution and secondary precipitates. *8th Washington Hydrogeology Symposium*, April 26-28, Tacoma, WA.

Wang, G, and Um. W. (2012) – Facilitated contaminant transport by remobilization of Sr containing colloid-sized secondary precipitates in Hanford site subsurface. *The 243rd ACS National meeting*, March 25-29, San Diego, California.

Other references cited.

Kaplan, D.I., Bertsch, P.M., Adrlano, D.C., Miller, W.P. (1993) – Soil-borne mobil colloids as influenced by water flow and organic carbon. Environ. Sci. Technol., 27, 1193-1200.

Roy, S.B., Dzombak, D.A., (1997) – Chemical factors influencing colloid-facilitated transport of contaminants in porous media. Environ. Sci. Technol., 31, 656-664

Gamerdinger, A.P., Kaplan, D.I. (2001) – Physical and chemical determinants of colloid transport and deposition in water-unsaturated sand and Yucca Mountain tuff material. Environ. Sci. Technol., 35, 2497-2504

Um, W., Papelis, C. (2002) –. Geochemical effects on colloid-facilitated metal transport through zeolitized tuffs from the Nevada test site. Environmental Geology, 43, 209-218

Ryan, J.N., Gschwend, P.M. (1994) – Effects of ionic strength and flow rate on colloid release: Relating kinetics to interface potential energy. J. of colloid and interface science, 164, 21-34.

Zhuang, J., McCarthy, J. F., Tyner, J.S., Perfect, E., Flury, M.(2007) – In Situ Colloid Mobilization in Hanford Sediments under Unsaturated Transient Flow Conditions: Effect of Irrigation Pattern. Environ. Sci. Technol., 41, 3199-3204.